Heterogeneity of Receptor Function in Colon Carcinoma Cells Determined by Cross-talk between Type I Insulin-like Growth Factor Receptor and Epidermal Growth Factor Receptor

Yi Peter Hu,[1] Sandip B. Patil,[3] Michelle Panasiewicz,[2] Wenhui Li,[3] Jennie Hauser,[2] Lisa E. Humphrey,[1] and Michael G. Brattain[1]

[1]Eppley Institute for Research in Cancer and Allied Diseases, University of Nebraska Medical Center, Omaha, Nebraska; [2]Department of Pharmacology and Therapeutics, Roswell Park Cancer Institute, Buffalo, New York; and [3]Department of Surgery, University of Texas Health Science Center at San Antonio, San Antonio, Texas

Abstract

This study identifies a novel cross-talk paradigm between the type I insulin-like growth factor receptor (IGF1R) and epidermal growth factor receptor (EGFR) in colon cancer cells. IGF1R activation by ligand exposure in growth factor–deprived cells induces Akt activation in the FET, CBS, and GEO colon cancer cell lines. Investigation of IGF1R-mediated signaling pathways using small interfering RNA approaches indicated that, as expected, phosphatidylinositol 3′-kinase (PI3K) was activated by IGF1R. Mitogen-activated protein kinase (MAPK) activity as reflected by phospho-extracellular signal-regulated kinase (ERK) induction was not significantly activated until later times following release of these cells from growth factor deprivation stress. The appearance of phospho-ERK was proximal to EGFR activation. Treatment of cells with the PI3K inhibitor LY294002 before release from stress resulted in a concentration-dependent loss of EGFR activation, whereas treatment with the MAPK inhibitor PD98059 did not block EGFR activation, indicating that EGFR activation was downstream of the IGF1R/PI3K pathway. PD98059 inhibition of MAPK was associated with a concentration-dependent reduction in EGFR-mediated phospho-ERK. EGFR inhibitor blocked induction of phospho-ERK, showing that MAPK activity was a consequence of EGFR-mediated signaling. On the other hand, a small-molecule IGF1R inhibitor, PQIP, blocked Akt phosphorylation. The divergent signaling functions of IGF1R and EGFR suggested the potential for synergism by a combination of therapy directed at the two receptors. Combination treatment with PQIP and EGFR inhibitor Tarceva resulted in synergistic effects as indicated by combination index analysis in all three cell lines tested. [Cancer Res 2008;68(19):8004–13]

Introduction

The type I insulin-like growth factor receptor (IGF1R) signaling pathway is an important growth-regulatory pathway that is prevalent in a variety of cancer types, including colon cancer (1–3). Both IGF1 and insulin are capable of binding and activating the IGF1R. Ligand binding induces receptor autophosphorylation at the tyrosine kinase domains, which in turn phosphorylates the tyrosine residues on various substrates and adaptor proteins (4). Two of the key substrates of the IGF1R are the insulin receptor substrate 1 (IRS1) and the src homology collagen-like (Shc) docking protein. When IRS1 is phosphorylated, it can recruit other signaling messengers, including phosphatidylinositol 3′-kinase (PI3K), leading to downstream activation of diverse signaling cascades. The IGF1R can also activate Shc protein, which leads to the activation of the mitogen-activated protein kinase (MAPK). The PI3K and MAPK influence key cell survival and proliferation events (2, 3, 5, 6).

Previous work had shown that IGF1R activation is crucial for the mitogenic and transforming activity of the epidermal growth factor receptor (EGFR; ref. 7). However, it was not clear whether IGF1R was upstream or downstream of EGFR in this cooperative relationship (8). We determined that the IGF1R was upstream of EGFR during mitogenesis and mediated cell cycle reentry from a quiescent state through the induction of transforming growth factor α (TGFα)-mediated activation of the EGFR (9).

The FET colon carcinoma cell line is derived from an early-stage colon tumor. This cell line is poorly tumorigenic, well differentiated, and has been characterized as growth factor dependent because FET cells require exogenous growth factor supplementation, including transferrin and insulin, in serum-free medium for proliferation (10–13). Previous studies showed that the mitogenicity of insulin (at the concentrations used) in cultures of these cells is not through the insulin receptor but instead through the IGF1R. Moreover, IGF1R activation led to the subsequent activation of the EGFR, which then stimulated reentry into the cell cycle by cells in G_0 (14). A similar dependence on IGF1R activation has been shown for CBS and GEO cell lines as well.

Major signaling pathways activated by the IGF1R and EGFR include the PI3K and MAPK pathways. Because these receptors seem to be so similar in their signaling mechanisms, it was of interest to study their cooperative mechanism in more detail. Previous studies had not addressed the signaling mechanisms underlying this cooperative relationship between the two receptors. Consequently, we asked whether they activate the same pathways in the context of cross-talk, thereby contributing to the overall amplitude of signaling, or whether they stimulated different pathways that contributed to different cellular functions. Here, we show that inhibition of the IGF1R-mediated activation of the PI3K pathway results in the inhibition of EGFR activation. The MAPK pathway does not seem to be directly involved with the activation of IGF1R. However, IGF1R has an indirect role in the activation of the MAPK pathway as MAPK is dependent on EGFR signaling in these cells. Moreover, MAPK is a key determinant of the biological effect of the IGF1R and EGFR cross-talk as

Note: Y.P. Hu and S.B. Patil contributed equally to this work.

Requests for reprints: Michael G. Brattain, Eppley Institute for Research in Cancer and Allied Diseases, University of Nebraska Medical Center, 987696 Nebraska Medical Center, Omaha, NE 68198-7696. Phone: 402-559-4902; Fax: 402-559-3739; E-mail: mbrattain@unmc.edu.

doi:10.1158/0008-5472.CAN-08-0280

EGFR-mediated MAPK activity is required for DNA synthesis in this group of cell lines. Moreover, a combination of IGF1R and EGFR inhibition achieved synergy of growth inhibition in all three cell lines.

Materials and Methods

Cell culture. The human colon carcinoma cell lines were originally developed from primary tumors and have been extensively characterized (10–14). Cells are maintained in a chemically defined serum-free medium consisting of McCoy's 5A medium (Sigma-Aldrich) supplemented with amino acids, pyruvate, vitamins, antibiotics, and the growth factors transferrin (4 μg/mL; Sigma-Aldrich) and insulin (20 μg/mL; Sigma-Aldrich) and EGF (10 ng/mL; R&D Systems). Supplemented McCoy's medium ("SM") is McCoy's 5A medium supplemented with antibiotics and nutrients but lacking any growth factors. "TI" medium is SM plus transferrin and insulin, whereas the normal culture medium ("TIE" or "SF") is TI medium plus EGF. FET cells were adapted to TI medium. Cultures were maintained at 37°C in a humidified atmosphere of 5% CO_2. Cells were routinely subcultured with a 0.25% trypsin (Invitrogen) in Joklik's medium (Invitrogen) containing 0.1% EDTA.

Antibodies, immunoblot, and immunoprecipitation. Anti-EGFR polyclonal, anti-phospho-EGFR Y1173, anti-PI3K (p85), anti-IRS1 polyclonal, anti-IGF1Rβ polyclonal, anti-extracellular signal-regulated kinase (ERK) polyclonal, and anti-phospho-ERK monoclonal antibodies were from Santa Cruz Biotechnology. Anti-phospho-IGF1R antibody (15) was obtained from Calbiochem. Anti-phosphotyrosine RC-20 antibody (for Western blot) and anti-phosphotyrosine PY20 monoclonal antibody (for immunoprecipitation) were from BD Biosciences. Anti-phospho-EGFR Y1068 and Y1086, anti-phospho-Akt Ser^{473}, anti-Akt polyclonal, anti-activated p38, and anti-caspase-7 polyclonal antibodies were from Cell Signaling Technology, Inc. Anti-actin and anti-tubulin antibodies were from Sigma-Aldrich. Immunoblot and immunoprecipitation were carried out as previously described (16).

Cell lysate preparation. Cultured colon carcinoma cells (FET, GEO, and CBS) were allowed to grow to 80% to 90% confluence in 100-mm culture plates or, in the case of inhibitor studies, six-well tissue culture plates. The medium was changed to SM medium and the cells were made quiescent through nutrient and growth factor deprivation for 5 d. Cells were then released in TI/TIE medium (growth factor and nutrient replenishment) or SM (nutrient replenishment alone) and harvested at various time points as indicated in the figures. In inhibitor studies, cells were treated with various concentrations of inhibitors on release from quiescence and were harvested at the time points indicated in the figures for dose-response studies. Cells were washed in PBS and collected in lysis buffer [50 mmol/L Tris (pH 7.4), 100 mmol/L NaCl, 1% NP40, 2 mmol/L EDTA, 0.1% SDS, 50 mmol/L NaF, 10 mmol/L Na_3VO_4, 1 mmol/L phenylmethylsulfonyl fluoride, 25 μg/mL β-glycerophosphate, and one protease inhibitor cocktail tablet from Roche]. Crude cell lysates were passed through a 21-gauge needle to shear DNA and lysed for 30 min at 4°C. Cell lysates were then cleared by centrifugation at 21,000 rpm for 15 min at 4°C and protein concentrations were determined by the Pierce bicinchoninic acid protein assay (Pierce Biotechnology).

[^{3}H]thymidine incorporation assay (mitogenesis). Confluent FET cells were growth arrested by growth factor and nutrient deprivation for 5 d in SM medium and subsequently released from growth arrest by providing fresh nutrients (SM) or nutrients and growth factors (TI). Cells were pulsed for 1 h with 25 μCi [^{3}H]thymidine (GE Healthcare Bio-Sciences). The free thymidine was removed and the cells were washed with ice-cold PBS. Trichloroacetic acid was added and the precipitated radioactivity was solubilized in 0.2 mol/L NaOH solution. Radioactive incorporation into DNA was then determined (17). For inhibition of mitogenesis studies, cells were treated with various concentrations of inhibitors at the time of release from quiescence. Cells were then pulsed and assayed for radioactive incorporation as described above.

IGF1R small interfering RNA transfection and knockdown of p110α protein using small interfering RNA. Silencer validated IGF1R small interfering RNA (siRNA) was obtained from Ambion, whereas the PIK3CA SMARTpool consisting of four siRNA duplexes (18) was used against PIK3CA, and the scrambled control siRNA was from Qiagen. FET cells were plated in antibiotic-free "10F" medium [supplemental McCoy medium containing 10% fetal bovine serum (Mediatech, Inc.)] at a density of 200,000 per well in six-well plates. The cells were allowed to attach overnight. 10F media were changed once 30 min before transfection. The transfection was carried out using Lipofectamine 2000 from Invitrogen and was performed according to the manufacturer's instructions. The plates were washed once with TI medium 5 h after transfection and replenished with TI medium. The culture media (TI) were changed again after 48 h. The cell lysates were collected 72 h after transfection.

DNA fragmentation assay (Cell Death Detection ELISA). FET cells were plated at a density of 10,000 per well in SF medium in 96-well plates and allowed to attach overnight at 37°C. The cells were changed to TI medium 24 h later and treated with either PD98059 or LY294002 at the indicated concentrations for another 72 h at 37°C. DNA fragmentation was detected by the Roche Cell Death Detection ELISA kit according to the manufacturer's instructions (Roche).

Cell proliferation inhibition assay. Cell proliferation was evaluated by 3-(4,5-dimethylthiazol-2-yl)-2,5-diphenyltetrazolium bromide (MTT; Sigma) assay as described earlier (19). Briefly, FET, GEO, and CBS cells were seeded in 96-well tissue culture plates (Costar) at 8,000 per well per 100 μL. Cells were allowed to attach overnight and then treated with 100 μL serial concentrations of PQIP, Tarceva, and the combination of PQIP plus Tarceva at constant ratios indicated in the text. After 72 h of drug exposure at 37°C, MTT solution (50 μL, 2 mg/mL) was added to each well. The reaction was stopped by removal of MTT after 2 h of incubation at 37°C. DMSO (150 μL) was added to dissolve formazan crystals. Absorbance at 570 nm was recorded using a 96-well plate reader.

Combination index value analysis. The combination index (CI) was determined by the Chou and Talalay method, a well-established mathematical analysis to determine the pharmacologic interaction between two drugs (20). The CI value of nonexclusive drugs is calculated by the following formula:

$$CI = (Da + Db)/(Dxa + Dxb) + DaDb/DxaDxb$$

where Da and Db are the doses of drug A and B that inhibit X% of cell proliferation as single drugs, and Dxa and Dxb are doses of drug A and B that inhibit X% of cell growth in a combination regimen. CI = 1 indicates an additive effect of the two drugs and the CI formula is the same as a traditional isobologram equation. Synergism is defined as more than the expected additive effect yielding a CI < 1, whereas antagonism has a CI > 1. CI values were analyzed using CalcuSyn software (Biosoft) and previously described (19, 21). Inputs for the equation below are the concentrations of single inhibitors, the combination doses at fixed ratios, and the fractional inhibition [fraction affected (Fa)] of single drugs and combinations. The equation is given by $Fa = (A_{570}\ \text{control} - A_{570}\ \text{treated})/A_{570}\ \text{control}$, whereas the fraction of unaffected cells (Fu) = 1 − Fa.

Results

PI3K is downstream of the IGF1R-mediated induction of TGFα in colon carcinoma cells. FET cells were growth arrested by nutrient and growth factor deprivation as described in Materials and Methods. IGF1R expression levels remain constant during growth arrest and do not differ after release from growth arrest by TI medium. However, the IGF1R is activated within 5 min of release from quiescence by TI. On the other hand, the activation of the EGFR is not significantly induced until 1 h after TI release from growth arrest (Fig. 1*A*). This observation was consistent with previous studies showing that EGFR expression was not observed until this time point (9, 14).

In contrast to release from growth arrest by TI medium, release in medium without an IGF1R ligand (insulin in this study) results in only modest DNA synthesis and does not result in the activation of

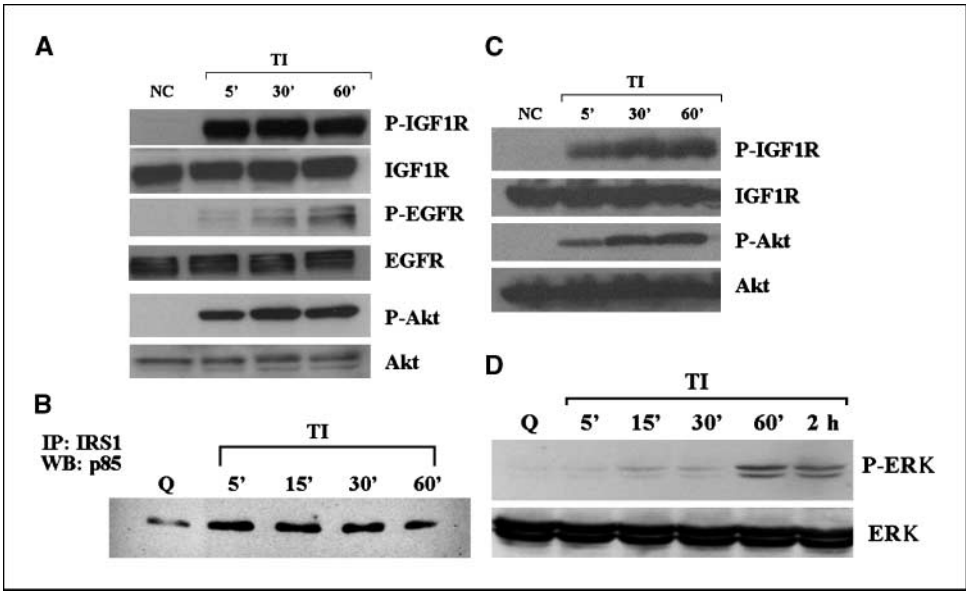

Figure 1. Receptor signaling activation after TI release. *A,* detection of IGF1R and EGFR activation after release: FET cells were starved for 5 d in growth factor–null medium and then stimulated to reenter the cell cycle by addition of medium containing transferrin and insulin (TI) for 5, 30, and 60 min as indicated. Lysates were separated by SDS-PAGE. The proteins were transferred onto nitrocellulose and subjected to antibodies for immunoblot analysis. *NC,* no change. PI3K pathway activation on TI release from quiescence: lysates collected after TI release from quiescence were subjected to SDS-PAGE and blotted for phospho-Akt (*P-Akt*) antibody. The blot was stripped in stripping buffer [62.5 mmol/L Tris-HCl (pH 6.8), 100 mmol/L β-mercaptoethanol, 2% SDS, 30 min at 50°C] and reblotted for Akt antibody. *P-IGF1R,* phospho-IGF1R; *P-EGFR,* phospho-EGFR. *B,* FET cell lysates (200 μg) from different time points after TI release were immunoprecipitated (*IP*) with IRS1 antibody, the immunocomplex was then incubated with protein A-agarose, the pellet was washed and eluted using lysis buffer, and the protein was resolved by 7.5% SDS-PAGE and then visualized by immunoblotting the p85 subunit of PI3K. *WB,* Western blot. *C,* detection of IGF1R and Akt activation after release in CBS cells: similar protocols as described above were applied to CBS cells. *D,* ERK activation: FET cell lysates from different time points after TI release were subjected to SDS-PAGE and blotted for phospho-ERK (*P-ERK*). The blot was stripped and reblotted for total ERK antibody. *Q,* quiescence.

the IGF1R (9, 13). This indicates that IGF1R plays an important role in the regulation of cell cycle reentry in FET cells. We next investigated IGF1R-mediated signaling pathways involved in this function. To determine the mechanism by which the IGF1R stimulates autocrine TGFα (9), activation kinetics of two key signaling pathways activated by the IGF1R (PI3K and MAPK pathways) were determined. A dramatic increase in Akt phosphorylation was detected after release from quiescence (Fig. 1*A*).

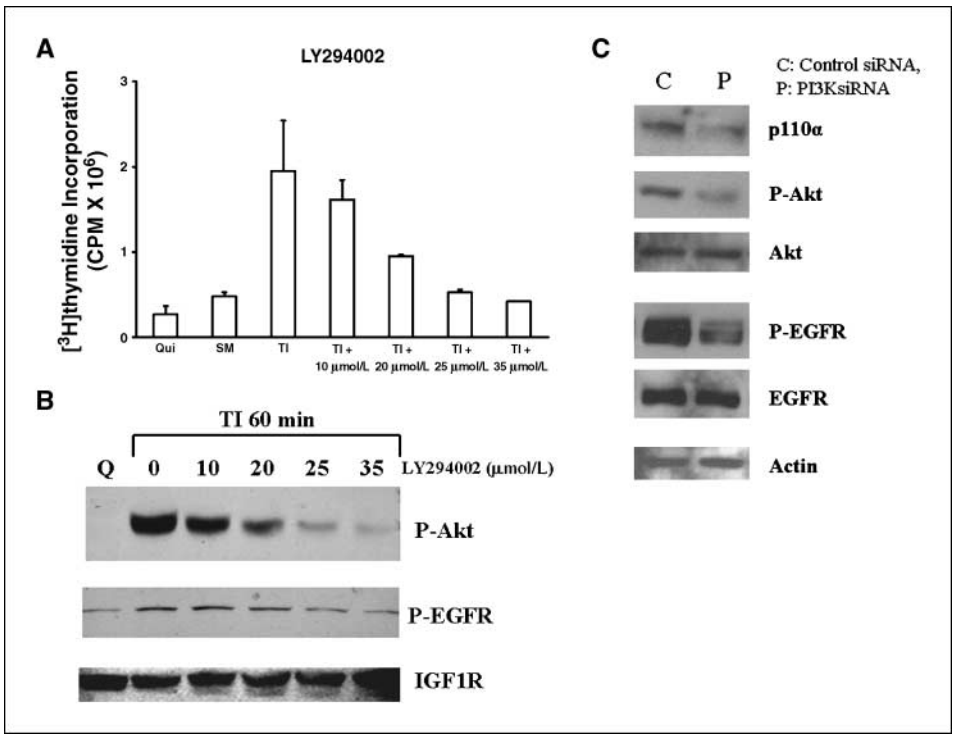

Figure 2. PI3K inhibitor LY294002 treatment. *A,* the mitogenesis assay was performed as described in Materials and Methods. FET cells were treated with increasing concentrations of LY294002 before release and grown for 22 h. Cells were then pulsed with 25 μCi of tritiated thymidine for 1 h to analyze for DNA synthesis. *Columns,* mean ($n = 3$); *bars,* SD. *B,* quiescent FET cells were treated with various concentrations of LY294002 for 30 min before TI release (60 min) and the lysates obtained were analyzed for the activation of Akt and EGFR. *C,* FET cells were transfected with PIK3CA siRNA to down-regulate p110α as described in Materials and Methods. Lysates were analyzed for p110α, the activation of Akt, and EGFR. Actin was used as a loading control.

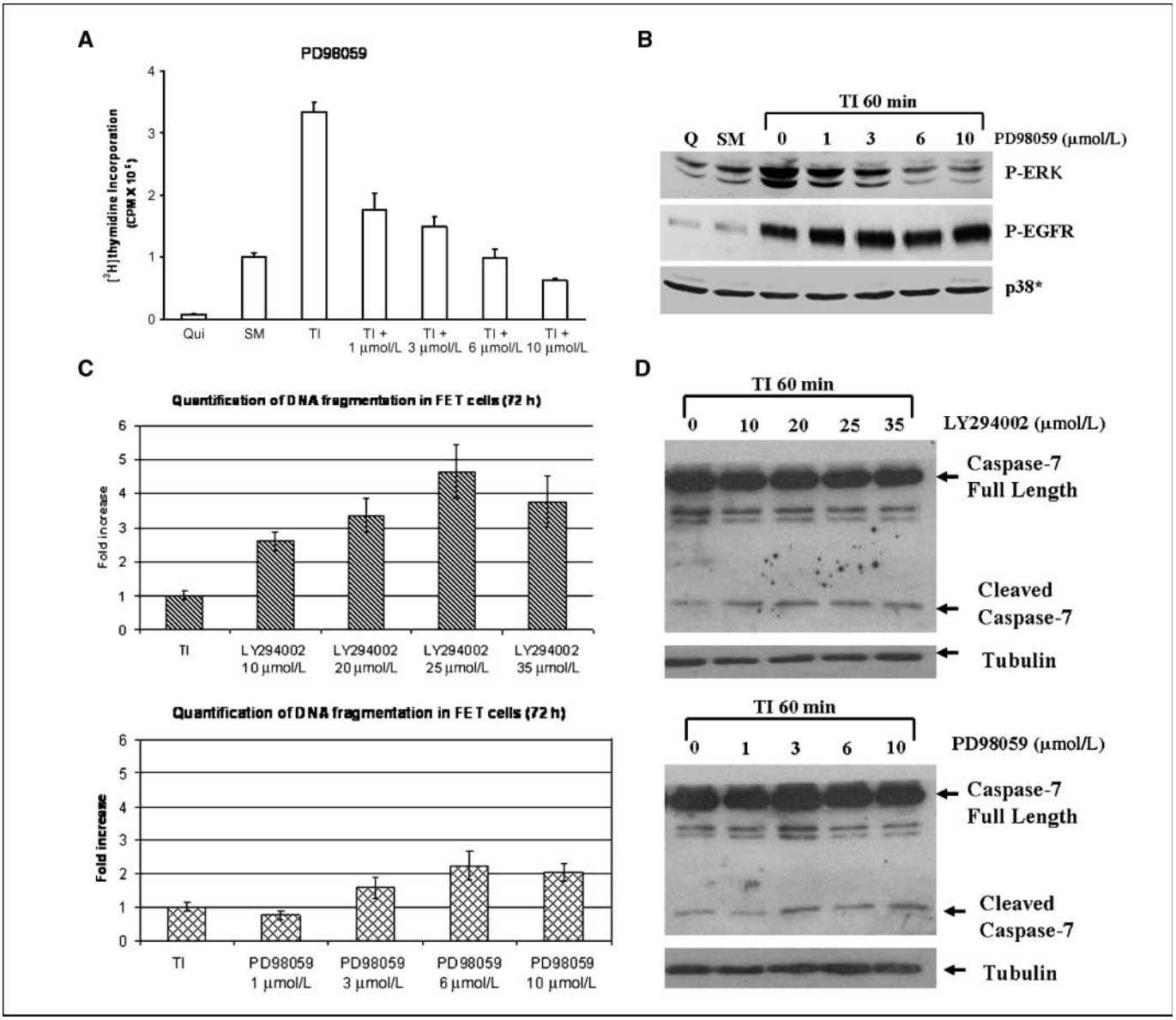

Figure 3. Inhibition of MAPK activation by MEK inhibitor PD98059. *A,* the mitogenesis assay was performed as described in Materials and Methods. Similar to LY294002 treatment, FET cells were treated with increasing concentrations of PD98059. *Columns,* mean ($n = 3$); *bars,* SD. *B,* quiescent cells were treated with various concentrations of PD98059 as indicated for 30 min before TI release (60 min) and the lysates obtained were analyzed for the activation of ERK, p38, and EGFR. *C* and *D,* contributions of PI3K and MAPK pathways to cell survival: FET cells were seeded at 10,000 per well in 96-well plates and allowed to adhere overnight. The next day, media were changed to TI medium and cells were treated with either PD98059 (1, 3, 6, and 10 μmol/L) or LY294002 (10, 20, 25, and 35 μmol/L) as described in Materials and Methods. *C,* Death Detection ELISA assays were performed and absorbance was measured at 405 nm. *Columns,* mean ($n = 3$); *bars,* SD. *D,* quiescent FET cells were treated with either PD98059 (1, 3, 6, and 10 μmol/L) or LY294002 (10, 20, 25, and 35 μmol/L) with TI release and whole-cell lysates were resolved by SDS-PAGE and immunoblotted with caspase-7 antibody. Anti-tubulin antibody was used as a loading control.

Furthermore, immunoprecipitation of IRS1, an IGF1R substrate, and the p85 subunit of the PI3K indicated an increase of IRS1-p85 complex formation after 5 min of release in TI medium (Fig. 1*B*). These lines of evidence indicate that PI3K is downstream of IGF1R activation. This phenomenon is not restricted to the FET cell line model as we observed similar IGF1R/Akt activation after 5 min of release in TI medium in growth-arrested CBS (Fig. 1*C*) and GEO (data not shown) cells. Unlike the kinetics of PI3K activation, very little MAPK activity (as reflected by ERK activation) was observed until 1 h after TI release (Fig. 1*D*). This time point corresponds to the time at which the EGFR is significantly activated, suggesting that the bulk of MAPK activity observed may be a consequence of EGFR signaling and that IGF1R was not significantly contributing directly to the MAPK activation.

Inhibition of PI3K pathway blocks EGFR activation. FET cells were treated with the PI3K inhibitor LY294002 to block the PI3K pathway (22). Mitogenesis assays of LY294002-treated cells showed that 25 μmol/L LY294002 inhibited DNA synthesis to levels comparable with those observed on release in the absence of insulin (SM; Fig. 2*A*). We used the loss of Akt activation as a marker of PI3K pathway blockade because this molecule is downstream of PI3K. Because robust EGFR activation begins at 60 min following TI release, we performed the assays at this time point. Concentration-dependent inhibition of Akt activation by

LY294002 similar to that of inhibition of mitogenesis was observed (Fig. 2*B*).

If the PI3K pathway is involved in the IGF1R-mediated induction of EGFR activation, then inhibition of this pathway should block the activation of the EGFR. To test this hypothesis, we used two approaches. First, we treated cells with LY294002 and assayed for EGFR activation. We found that treatment of LY294002 results in the inhibition of EGFR activation (Fig. 2*B*). We also performed transfection of siRNA to the p110α subunit of PI3K in FET cells. The transfection knocked down PIK3CA protein expression, resulting in down-regulation of phospho-Akt and inhibition of EGFR activation (Fig. 2*C*). Thus, the activation of the PI3K pathway is required for the induction of EGFR activation during mitogenesis.

Inhibition of MAPK pathway does not affect EGFR activation. To block the activation of the MAPK pathway, we used the MAPK/ERK kinase (MEK) inhibitor PD98059 (23). We first performed a mitogenesis assay to determine the suitability of the concentrations selected. Figure 3*A* shows that 6 to 10 μmol/L of PD98059 inhibit DNA synthesis to SM levels. Treatment of FET cells with PD98059 also resulted in a concentration-dependent inhibition of ERK activity at 1 h after release from growth arrest (Fig. 3*B*). We determined the effect of PD98059 on p38, a protein closely related to MAPK, to ensure selectivity for the ERK pathway.

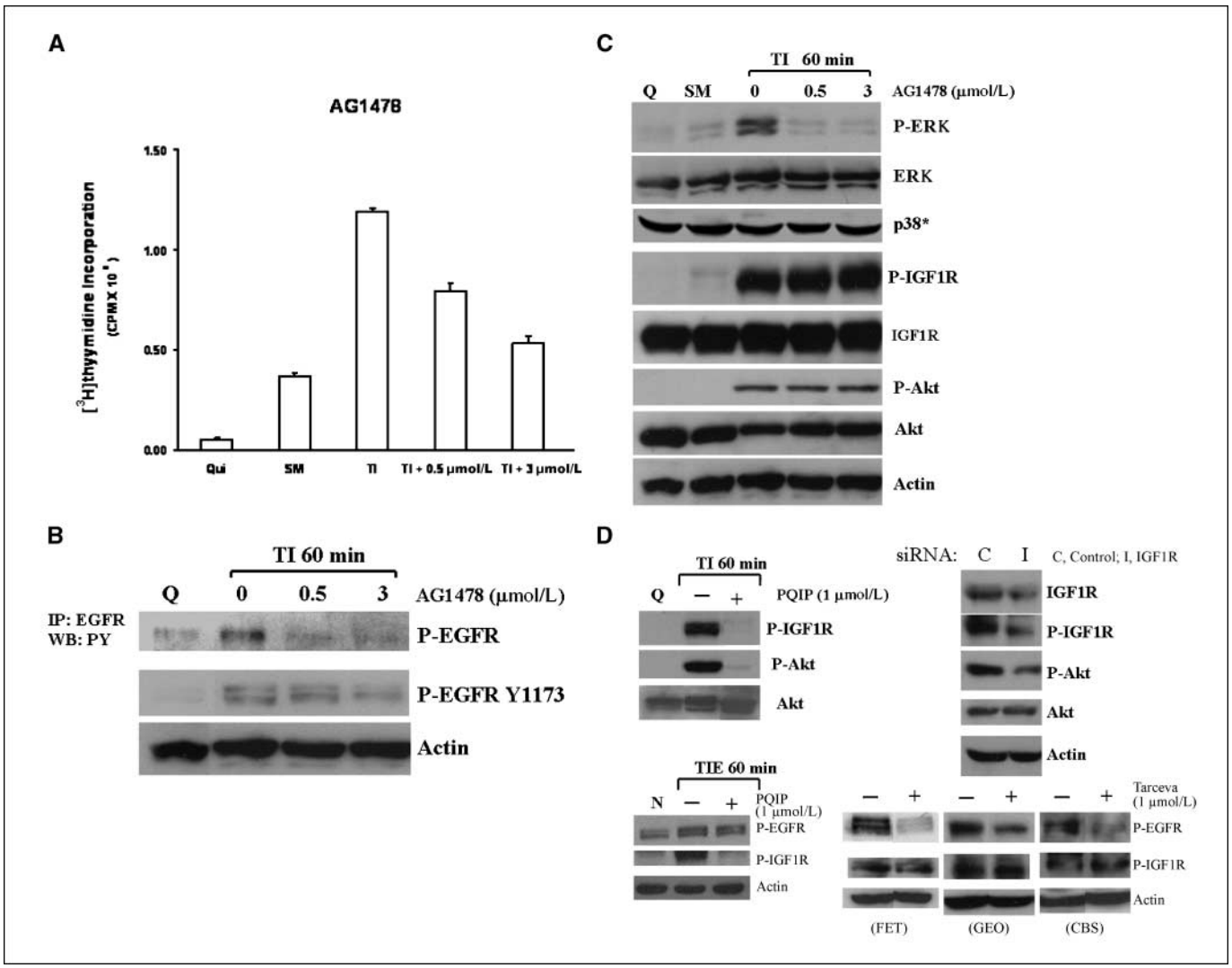

Figure 4. Inhibition of EGFR by AG1478 blocks MAPK activation. *A,* the mitogenesis assay was performed as described in Materials and Methods. Quiescent FET cells were treated with increasing concentrations of AG1478 as indicated. *Columns,* mean (n = 3); *bars,* SD. *B,* cells were treated with various concentrations of AG1478 for 30 min before TI release (60 min) and the lysates were incubated with the EGFR antibody. The antibody-antigen complex was then precipitated with protein A-agarose and resolved by 7.5% SDS-PAGE followed by immunoblotting with the phosphotyrosine antibody RC-20. EGFR activation was also detected by using an anti-phospho-EGFR Y1173 antibody (Santa Cruz Biotechnology). *C,* lysates were also analyzed for the activation of ERK, p38, and Akt. IGF1R phosphorylation was measured either by an anti-phospho-IGF1R antibody (shown) or by incubating cell lysates with PY20 antibody and the immunocomplex was then precipitated with protein A-agarose and resolved by 7.5% SDS-PAGE followed by IGF1R immunoblotting (data not shown). *D,* inhibition of IGF1R activation down-regulated phospho-Akt: quiescent cells were treated with 1 μmol/L PQIP for 30 min before TI release (60 min) and the lysates obtained were analyzed for the activation of IGF1R and Akt. Total Akt was also used as a loading control. FET cells were transfected with IGF1R siRNA to down-regulate IGF1R as described in Materials and Methods. Lysates were analyzed for IGF1R and the activation of IGF1R and Akt. Actin was used as a loading control. PQIP does not block EGFR phosphorylation in EGF-stimulated cells: cells were treated with 1 μmol/L PQIP for 30 min before TIE release (60 min) and the lysates obtained were analyzed for the activation of IGF1R and EGFR. Actin was used as a loading control. *N,* no change. Tarceva fails to affect IGF1R signaling: cells were treated with 1 μmol/L Tarceva for 30 min and the lysates obtained were analyzed for the activation of EGFR and IGF1R.

Table 1. IC_{50} values of PQIP and Tarceva and PQIP + Tarceva at constant ratios in FET, CBS, and GEO cells

IC_{50} value*	PQIP (μmol/L)			Tarceva (μmol/L)		
Treatment	FET	CBS	GEO	FET	CBS	GEO
PQIP single drug	0.28 ± 0.14	0.64 ± 0.12	0.24 ± 0.14	NA	NA	NA
Tarceva single drug	NA	NA	NA	3.33 ± 0.15	9.91 ± 1.29	0.99 ± 0.10
PQIP + Tarceva (1:9 for FET, 1:10 for CBS, and 1:2 for GEO)	0.025 ± 0.005	0.081 ± 0.025	0.044 ± 0.029	0.223 ± 0.048	0.806 ± 0.255	0.089 ± 0.057

Abbreviation: NA, not available.
*IC_{50} values were determined from MTT data after 72 h of drug treatment by CalcuSyn software. Representative data of two repeated experiments were shown here.

PD98059 was selective for the ERK pathway as it did not inhibit p38 activation at the concentrations used (Fig. 3*B*). The role of the MAPK pathway in EGFR activation was then investigated with PD98059 treatment. The result shows that PD98059 does not inhibit EGFR activation (Fig. 3*B*). These data indicated that the MAPK pathway is not involved in the regulation of the EGFR activation.

PI3K pathway participates in cell survival. Because IGF1R-regulated PI3K activates EGFR through TGFα (9), and MAPK activation is subsequent to the activation of EGFR during mitogenesis, this raises the question of the function of the two receptors and the pathways activated by them. To address this issue, we performed DNA fragmentation assays and found that the selective PI3K inhibitor LY294002 induced apoptosis in FET cells grown in TI medium. Inhibition of activated Akt by 25 μmol/L LY294002 resulted in approximately a 5-fold increase of apoptosis as reflected by DNA fragmentation assays. On the other hand, MEK inhibition by PD98059 resulted in a more modest 2-fold induction of apoptosis (Fig. 3*C*). Caspase-7 cleavage assays confirmed that both inhibitors increased apoptosis in FET cells released in TI medium after growth factor deprivation stress (Fig. 3*D*). Thus, whereas PI3K plays a dominant role in cell survival, the MAPK pathway elicited by IGF1R-mediated EGFR activation also participates in the support of cell survival signaling.

Inhibition of EGFR blocks MAPK activation. The MAPK activation studies showed that ERK activation occurs at ~60 min following growth factor addition. This coincides with robust EGFR activation (Fig. 1). Taken together with the finding that inhibition of MEK does not inhibit EGFR activation (Fig. 3*B*), we hypothesized that MAPK activation is derived from EGFR activation. To test this, we treated FET cells with AG1478, a selective EGFR inhibitor that has been widely used as a tool in studying EGFR-mediated signal transduction (24–26). Cells were treated with various concentrations of AG1478 before release from quiescence. Figure 4*A* shows that at 0.5 μmol/L AG1478 inhibited the DNA synthesis of FET cells in TI medium. As observed in Fig. 4*B*, this concentration of AG1478 also blocks the activation of the EGFR at 1 h of release. We then treated FET cells with AG1478 and determined its effects on ERK activation at 1 h after release from growth arrest. AG1478 inhibited the activation of ERK that was observed at 1 h of release in TI in the absence of the inhibitor (Fig. 4*C*). This shows that MAPK activity is downstream of EGFR activation. AG1478 treatment did not affect the activation of p38 in this cell line (Fig. 4*C*). We assessed whether AG1478 treatment was inhibiting IGF1R activation. Again in Fig. 4*C*, the result shows the activation of IGF1R at 60 min of TI release in the presence of 0 to 5 μmol/L of AG1478. As expected, AG1478 does not affect IGF1R activation, thereby indicating selective effects on this tyrosine kinase receptor.

We next tested the role of EGFR on the activation of the PI3K pathway components. Figure 4*C* shows the lack of effect of AG1478 treatment on activated Akt levels. AG1478 does not show any inhibition of phospho-Akt at 0.5 μmol/L treatment, the concentration of the drug at which EGFR activation and DNA synthesis are inhibited. Moreover, higher AG1478 concentrations (5–20 μmol/L) did not inhibit activated IGF1R nor Akt phosphorylation but did effectively block ERK activation (data not shown), further indicating that PI3K/Akt axis plays a role downstream of IGF1R, whereas the MAPK pathway is under EGFR control in this cell line and is necessary for reentry into the cell cycle as reflected by indication of DNA synthesis.

Inhibition of IGF1R activation blocks Akt phosphorylation. Akt activation correlates with IGF1R activation after TI release described earlier in this study (Fig. 1). If PI3K activation is downstream of IGF1R, inhibition of IGF1R activation would result in blockade of Akt phosphorylation. To address this issue, we used two approaches. First, we used an IGF1R kinase inhibitor, PQIP (27), to inhibit IGF1R activation. PQIP (1 μmol/L) effectively inhibited IGF1R phosphorylation in FET cells released in TI medium, and the drug inhibited Akt phosphorylation as well (Fig. 4*D, top left*). However, this compound does not block EGFR phosphorylation in EGF-stimulated cells, confirming its specificity for IGF1R (Fig. 4*D, bottom left*). We next used IGF1R siRNA transfection to down-regulate IGF1R protein in FET cells. IGF1R siRNA effectively reduced IGF1R protein and activation level. Activation of Akt was also inhibited (Fig. 4*D, top right*), further indicating that PI3K/Akt axis is a downstream pathway of IGF1R in FET cells.

Growth inhibition of colon carcinoma cells by combination treatment of PQIP and Tarceva. Given the differences in function between IGF1R- and EGFR-activated pathways, we hypothesized that inhibition of both IGF1R and EGFR activation in colon cancer cells would be synergistic. We first determined the growth-inhibitory effects of PQIP, an IGF1R kinase inhibitor, and Tarceva (erlotinib; ref. 28), an EGFR kinase inhibitor, in colon cancer cells. Treatment of colon cancer cell lines FET, CBS, and GEO confirms that Tarceva fails to affect IGF1R signaling (Fig. 4*D, bottom right*). Drug concentrations and growth-inhibitory effects were analyzed by CalcuSyn software (Biosoft). IC_{50} values of PQIP and Tarceva

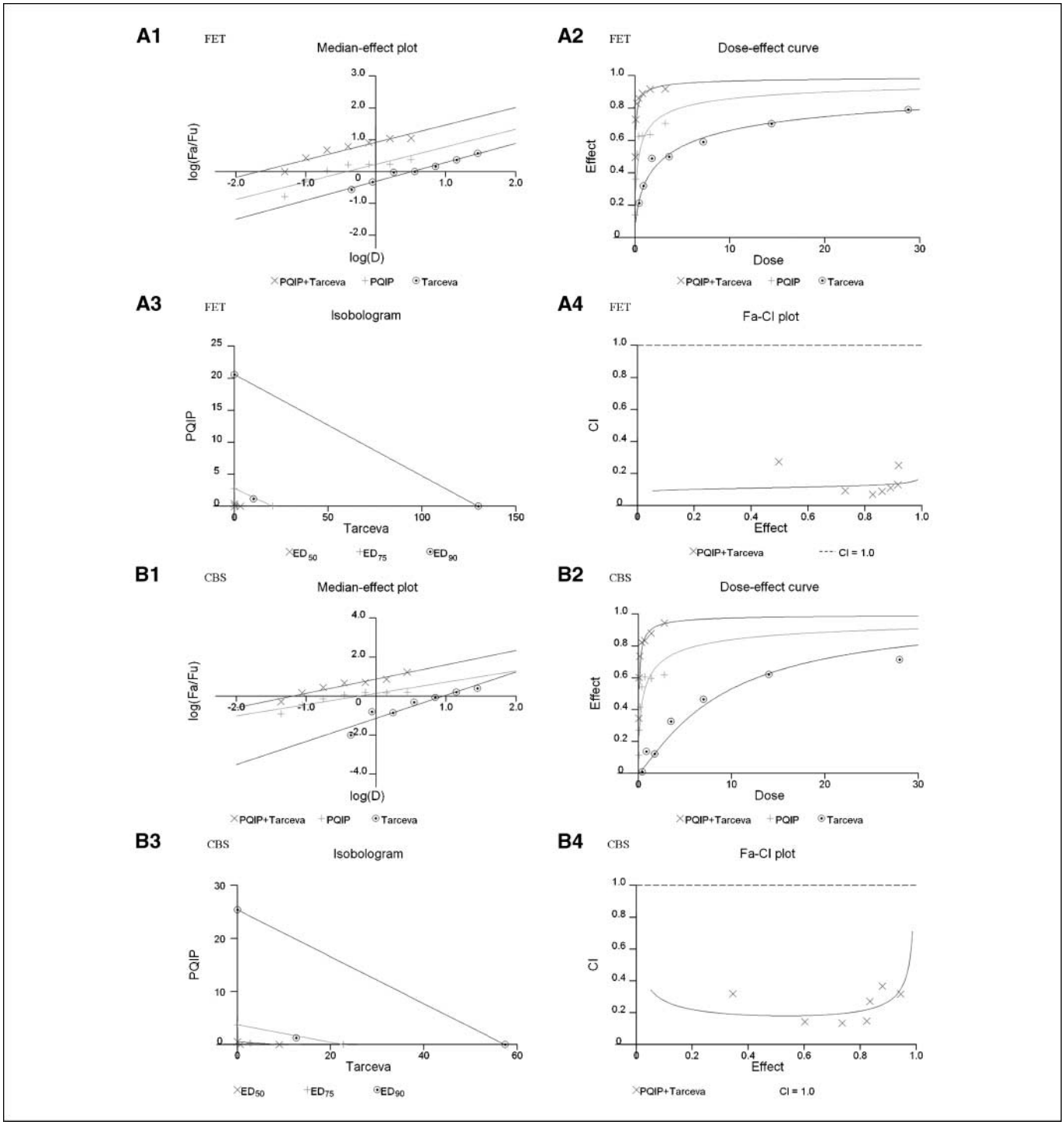

Figure 5. Synergistic effect of PQIP and Tarceva on growth inhibition in colon cancer cells. Growth inhibition of FET (*A*), CBS (*B*), and GEO (*C*) cells with PQIP, Tarceva, and PQIP + Tarceva at 1:9, 1:10, and 1:2 ratios was measured by MTT assay as described in Materials and Methods. *Top left,* the value of log (Fa/Fu) of PQIP + Tarceva was plotted against Tarceva concentrations used in the combinations in a median-effect plot; *top right,* the Fa for PQIP + Tarceva was plotted against the concentrations of PQIP used in the combinations in a dose-effect curve; *bottom left,* ED_{90}, ED_{75}, and ED_{50} values of PQIP and Tarceva are indicated on the *Y* axis and *X* axis of the isobologram, respectively. Concentrations of PQIP + Tarceva necessary to induce similar inhibitory effects are plotted on the isobologram in comparison with single drugs. *Bottom right,* CIs of PQIP + Tarceva at 1:9 (FET), 1:10 (CBS), and 1:2 (GEO) ratios were tested by CI analysis. CI value was analyzed by CalcuSyn software and plotted against Fa. Complete CI effect plot simulated by the software derived from the real data points is shown. An additive effect was reflected by CI = 1, a synergistic effect was reflected by CI < 1, and an antagonistic effect was reflected by CI > 1.

against FET cells were 0.28 and 3.33 μmol/L, respectively, as determined by 72-h drug exposure in MTT assays (Table 1). A fixed ratio of concentrations of PQIP/Tarceva at 1:9 was used in combination treatments based on the relative IC_{50} values. The concentrations of PQIP in the combination experiments ranged from 0.025 to 3.2 μmol/L, whereas the concentrations of Tarceva were correspondingly 9-fold higher. Growth inhibition effects were measured after 72 h of drug exposure and plotted as a

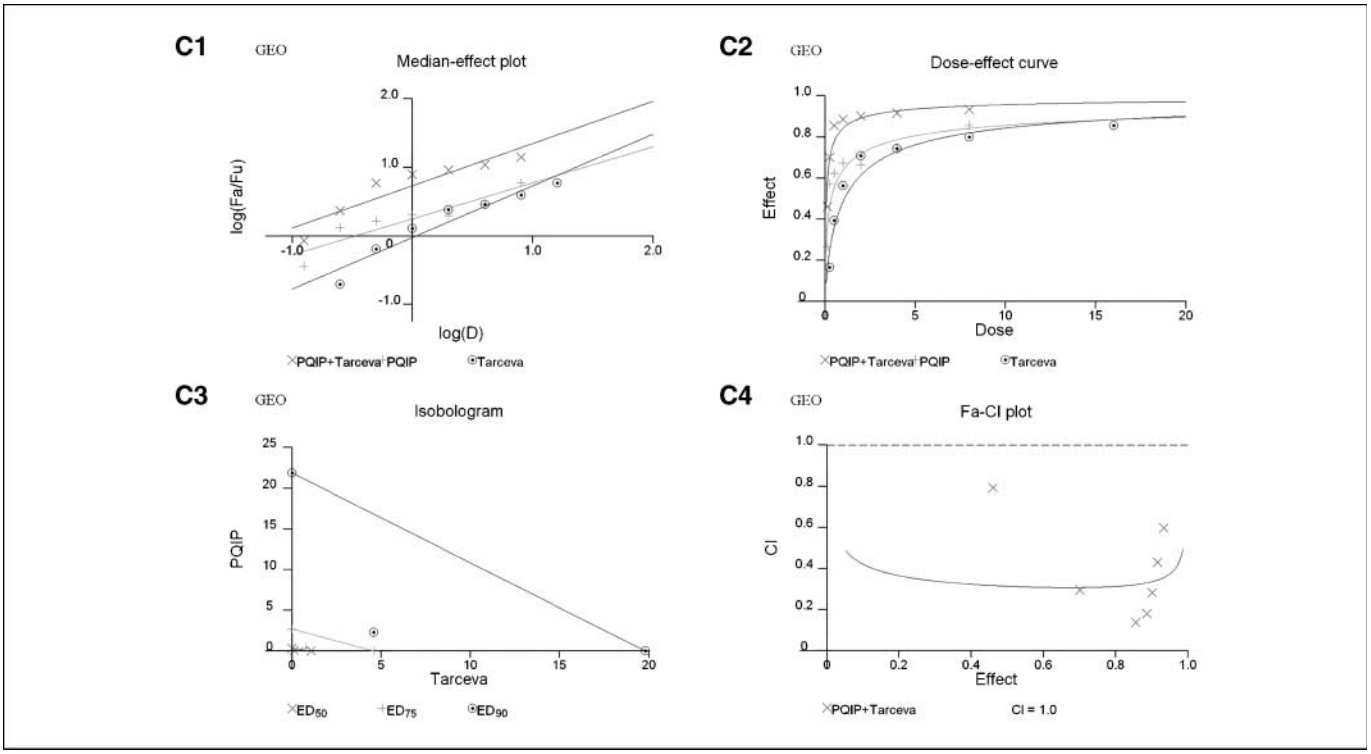

Figure 5 *Continued.*

median-effect plot as well as a dose-effect curve (Fig. 5*A*). The median-effect plot shows the linear relationship between the ratio of the Fa to the Fu, where Fu = 1 − Fa, and drug concentrations are in log values. IC_{50} values of single drugs or the combination regimens can be determined from the *X*-axis intersection value of the lines, where log (Fa/Fu) = 0. We observed a concentration-dependent inhibition of cell growth in both PQIP and Tarceva treatments alone as shown in the dose-effect curve. The shapes of the curves were different for PQIP and Tarceva, which reflected the different slopes in the median-effect plot. In both the median-effect plot and the dose-effect curve, the combination treatment of PQIP and Tarceva showed a parallel shift to the left in comparison with the single drugs when the inhibitory effect of combinations was plotted against the concentration of each drug. This indicated higher sensitivity of FET cells to the combination treatment than to the single drugs. Significantly, 11- and 15-fold decreases in the concentrations of PQIP and Tarceva, respectively, were sufficient for 50% inhibition of tumor cell proliferation at the 1:9 ratio combination compared with the IC_{50} value of either drug alone (Table 1). Moreover, the isobologram showed that the combination of PQIP plus Tarceva achieved more than an additive effect, as all of the data points from combinations fell below the line defined from the concentrations of single agents at 90% (ED_{90}), 75% (ED_{75}), and 50% (ED_{50}) inhibition, respectively (Fig. 5*A*). To further determine whether the inhibitory effects of targeting both IGF1R and EGFR kinase activity by the combination of PQIP plus Tarceva were synergistic, we analyzed the CI values of PQIP plus Tarceva using CalcuSyn software (Materials and Methods). Synergism (CI < 1) was observed at the combination concentrations used with a PQIP/Tarceva ratio of 1:9 (Fig. 5*A*). In fact, a strong synergistic effect (CI < 0.3) was determined at all combination concentrations tested in FET cells. Synergistic results were also observed in CBS and GEO cell lines (Table 1; Fig. 5*B* and *C*).

Discussion

Previously, we found that to obtain substantial reentry into the cell cycle from growth arrest in FET colon cancer cells, exogenous activation of IGF1R was necessary. The induction of autocrine TGFα-mediated EGFR activation in the G_1 phase of the cell cycle is an essential event for DNA synthesis in these cells, and the up-regulation of EGFR via the autocrine production of TGFα is an event lying downstream of the activation of the IGF1R (9, 14). TGFα was one of the first stimulatory growth factors to be described as having autocrine activity (29). The autocrine hypothesis was proposed to explain the growth advantage of malignant cells over their normal counterparts. Since the formulation of this hypothesis, it has become evident that normal cells show autocrine activities as well (30). Normal cells do not exhibit independence from exogenous growth factors for cell cycle reentry nor do they exhibit constitutive cell survival signaling in quiescence. The major growth advantage resulting from autocrine TGFα mediated by IGF1R activation here may be an enhanced ability to reenter the cell cycle from growth arrest in response to IGF1R ligands and to survive to conditions that are not growth permissive.

Earlier studies in Balb/3T3 cells have suggested that IGF1R activation is critical for cell cycle reentry and that the role of EGFR signaling is to produce sufficient IGF1R (7, 31). However, FET colon carcinoma cells present a novel cross-talk paradigm in which it is the TGFα/EGFR that is required for induction of mitogenesis, whereas IGF1R signaling leads to the activation of EGFR (9, 14). Another cross-talk paradigm has been shown between these two

receptors in COS7 cells. This example of cross-talk is mediated by autocrine heparin-binding EGF (HB-EGF; ref. 32). Activation of the IGF1R leads to EGFR activation via a mechanism involving matrix metalloproteinase–dependent release of HB-EGF in these cells. Thus, it seems that IGF1R-mediated EGFR activation can occur through the induction of a variety of EGFR ligands, and the cross-talk between IGF1R and EGFR shows great versatility in different cell lines.

Although the existence of cross-talk between IGF1R and EGFR has been described previously in the FET cell line (9, 14), the signaling pathways mediated by the IGF1R involved in this cross-talk had not been determined. Here, it has been shown for the first time that IGF1R-mediated EGFR activation through the induction of an autocrine TGFα loop is critically dependent on the activation of the PI3K pathway. This study also elucidates the signaling function of EGFR in the cross-talk. The delayed activation of the EGFR and MAPK pathway by TGFα induction may provide these cells with a mechanism for sustained cell survival signaling following an initial pulse of IGF1R-mediated PI3K activity. This initial burst of PI3K signaling provides the major survival support for the FET cells for escape from stress effects. MAPK also plays an important role in cell cycle reentry.

Our previous work indicated that either EGFR or ErbB2 can compensate for the inhibition of the other receptor when exposed to a single drug treatment with small-molecule antagonists (16, 19, 21). In contrast, targeting both receptors simultaneously provided synergistic effects with induction of apoptosis (16, 19). Interestingly, recent evidence also suggests a role for IGF1R signaling in the acquired resistance to drugs against EGFR or ErbB2. For example, IGF1R signaling has been reported to interfere with the growth-inhibitory action of the anti-ErbB2 monoclonal antibody trastuzumab (33, 34), and a correlation between IGF1R activation and acquired resistance to EGFR blockade was also shown (35, 36). In another study, coinhibition of EGFR and IGF1R sensitized human malignant glioma cells to CD95L-induced apoptosis (37). Thus, the strategy of targeting both IGF1R and EGFR to overcome acquired drug resistance would seem to have intriguing potential for human cancer therapy.

The presence of cross-talk between two potential therapeutic targets (EGFR and IGF1R) may be of particular importance in cancer therapy. Clinically applicable drugs against EGFR have been developed and inhibitors targeting IGF1R are emerging as well (15, 27, 38–44). Single drugs directed at molecular targets have had disappointing effect in the clinic (45). The tight interplay between IGF1R and EGFR signaling suggests that strategies against both receptors may be of value (37, 46–48). A recent study found that stimulation of head and neck cancer cells with either IGF or EGF resulted in IGF1R and EGFR heterodimerization, but only IGF caused activating phosphorylation of both receptors, indicating that the net effect of IGF-induced receptor signaling may rely, in part, on EGFR activation and/or IGF1R/EGFR scaffolding interactions. They also found that combined treatment with a human anti-IGF1R antibody A12 and the EGFR blocking antibody C225 was more effective at reducing cell proliferation and migration than either agent alone (49). In light of these developments, our findings provide an example that the TGFα autocrine loop can be activated by PI3K via IGF1R signaling induction and that MAPK can be activated subsequently by the activation of EGFR. Furthermore, we showed that combination treatment of IGF1R and EGFR kinase inhibitors resulted in synergy of growth inhibition in three human colon cancer cell lines (Table 1; Fig. 5). This implies that the heterogeneity of cross-talk between EGFR and IGF1R displays distinct mechanisms even in the same cell line in terms of regulating malignant cell growth. Intriguingly, the IC_{50} of Tarceva is decreased 15-fold in combination with PQIP in FET cell line. Similar dramatic changes were found in CBS and GEO cell lines as well. The significant increase of Tarceva potency in combination with an IGF1R inhibitor indicated that inhibition of IGF1R activation sensitizes EGFR inhibition by Tarceva. Hence, targeting one receptor such as IGF1R will lead to reshuffling of the downstream signaling pathways, such as the PI3K pathway, and affect the other receptor and EGFR signaling, simultaneously or afterwards. Because the interactions of these signaling pathways involve both cell cycle reentry and cell survival, the phenotype of the tumor cells will eventually be changed and, in turn, alter drug sensitivity.

Disclosure of Potential Conflicts of Interest

No potential conflicts of interest were disclosed.

Acknowledgments

Received 2/20/2008; revised 7/7/2008; accepted 7/22/2008.

Grant support: NIH grants CA34432, CA54807, and P30CA036727.

The costs of publication of this article were defrayed in part by the payment of page charges. This article must therefore be hereby marked *advertisement* in accordance with 18 U.S.C. Section 1734 solely to indicate this fact.

We thank Carol Smith for technical assistance and Dr. Yunfei Zhou for assistance in CalcuSyn program.

References

1. Reinmuth N, Liu W, Fan F, et al. Blockade of insulin-like growth factor I receptor function inhibits growth and angiogenesis of colon cancer. Clin Cancer Res 2002; 8:3259–69.
2. Sachdev D, Yee D. The IGF system and breast cancer. Endocr Relat Cancer 2001;8:197–209.
3. Surmacz E. Function of the IGF-I receptor in breast cancer. J Mammary Gland Biol Neoplasia 2000;5:95–105.
4. Ullrich A, Gray A, Tam AW, et al. Insulin-like growth factor I receptor primary structure: comparison with insulin receptor suggests structural determinants that define functional specificity. EMBO J 1986;5:2503–12.
5. Peruzzi F, Prisco M, Dews M, et al. Multiple signaling pathways of the insulin-like growth factor 1 receptor in protection from apoptosis. Mol Cell Biol 1999;19: 7203–15.
6. Brodt P, Samani A, Navab R. Inhibition of the type I insulin-like growth factor receptor expression and signaling: novel strategies for antimetastatic therapy. Biochem Pharmacol 2000;60:1101–7.
7. Coppola D, Ferber A, Miura M, et al. A functional insulin-like growth factor I receptor is required for the mitogenic and transforming activities of the epidermal growth factor receptor. Mol Cell Biol 1994;14:4588–95.
8. Werner H, LeRoith D. The role of the insulin-like growth factor system in human cancer. Adv Cancer Res 1996;68:183–223.
9. Wang D, Patil S, Li W, Humphrey LE, Brattain MG, Howell GM. Activation of the TGFα autocrine loop is downstream of IGF-I receptor activation during mitogenesis in growth factor dependent human colon carcinoma cells. Oncogene 2002;21:2785–96.
10. Chantret I, Barbat A, Dussaulx E, Brattain MG, Zweibaum A. Epithelial polarity, villin expression, and enterocytic differentiation of cultured human colon carcinoma cells: a survey of twenty cell lines. Cancer Res 1988;48:1936–42.
11. Schlechte W, Brattain M, Boyd D. Invasion of extracellular matrix by cultured colon cancer cells: dependence on urokinase receptor display. Cancer Commun 1990;2:173–9.
12. Brattain MG, Howell G, Sun LZ, Willson JK. Growth factor balance and tumor progression. Curr Opin Oncol 1994;6:77–81.
13. Jiang D, Yang H, Willson JK, et al. Autocrine

transforming growth factor α provides a growth advantage to malignant cells by facilitating re-entry into the cell cycle from suboptimal growth states. J Biol Chem 1998;273:31471–9.
14. Wang D, Li W, Jiang W, Humphrey LE, Howell GM, Brattain MG. Autocrine TGFα expression in the regulation of initiation of human colon carcinoma growth. J Cell Physiol 1998;177:387–95.
15. Garcia-Echeverria C, Pearson MA, Marti A, et al. *In vivo* antitumor activity of NVP-AEW541—a novel, potent, and selective inhibitor of the IGF-IR kinase. Cancer Cell 2004;5:231–9.
16. Hu YP, Venkateswarlu S, Sergina N, et al. Reorganization of ErbB family and cell survival signaling after knock-down of ErbB2 in colon cancer cells. J Biol Chem 2005;280:27383–92.
17. Mulder KM, Brattain MG. Effects of growth stimulatory factors on mitogenicity and c-myc expression in poorly differentiated and well differentiated human colon carcinoma cells. Mol Endocrinol 1989;3:1215–22.
18. Wang J, Kuropatwinski K, Hauser J, et al. Colon carcinoma cells harboring PIK3CA mutations display resistance to growth factor deprivation induced apoptosis. Mol Cancer Ther 2007;6:1143–50.
19. Zhou Y, Brattain MG. Synergy of epidermal growth factor receptor kinase inhibitor AG1478 and ErbB2 kinase inhibitor AG879 in human colon carcinoma cells is associated with induction of apoptosis. Cancer Res 2005;65:5848–56.
20. Chou TC, Talalay P. Quantitative analysis of dose-effect relationships: the combined effects of multiple drugs or enzyme inhibitors. Adv Enzyme Regul 1984;22:27–55.
21. Zhou Y, Li S, Hu YP, et al. Blockade of EGFR and ErbB2 by the novel dual EGFR and ErbB2 tyrosine kinase inhibitor GW572016 sensitizes human colon carcinoma GEO cells to apoptosis. Cancer Res 2006;66:404–11.
22. Vlahos CJ, Matter WF, Hui KY, Brown RF. A specific inhibitor of phosphatidylinositol 3-kinase, 2-(4-morpholinyl)-8-phenyl-4H-1-benzopyran-4-one (LY294002). J Biol Chem 1994;269:5241–8.
23. Alessi DR, Cuenda A, Cohen P, Dudley DT, Saltiel AR. PD 098059 is a specific inhibitor of the activation of mitogen-activated protein kinase kinase *in vitro* and *in vivo*. J Biol Chem 1995;270:27489–94.
24. Li Y, Li M, Xing G, et al. Stimulation of the mitogen-activated protein kinase cascade and tyrosine phosphorylation of the epidermal growth factor receptor by hepatopoietin. J Biol Chem 2000;275:37443–7.
25. Zhang P, Wang YZ, Kagan E, Bonner JC. Peroxynitrite targets the epidermal growth factor receptor, Raf-1, and MEK independently to activate MAPK. J Biol Chem 2000;275:22479–86.
26. Grosse R, Roelle S, Herrlich A, Hohn J, Gudermann T. Epidermal growth factor receptor tyrosine kinase mediates Ras activation by gonadotropin-releasing hormone. J Biol Chem 2000;275:12251–60.
27. Ji QS, Mulvihill MJ, Rosenfeld-Franklin M, et al. A novel, potent, and selective insulin-like growth factor-I receptor kinase inhibitor blocks insulin-like growth factor-I receptor signaling *in vitro* and inhibits insulin-like growth factor-I receptor dependent tumor growth *in vivo*. Mol Cancer Ther 2007;6:2158–67.
28. Baselga J. Targeting the epidermal growth factor receptor: a clinical reality. J Clin Oncol 2001;19:41–4S.
29. de Larco JE, Todaro GJ. Growth factors from murine sarcoma virus-transformed cells. Proc Natl Acad Sci U S A 1978;75:4001–5.
30. Sporn MB, Todaro GJ. Autocrine secretion and malignant transformation of cells. N Engl J Med 1980;303:878–80.
31. Pietrzkowski Z, Lammers R, Carpenter G, et al. Constitutive expression of insulin-like growth factor 1 and insulin-like growth factor 1 receptor abrogates all requirements for exogenous growth factors. Cell Growth Differ 1992;3:199–205.
32. Roudabush FL, Pierce KL, Maudsley S, Khan KD, Luttrell LM. Transactivation of the EGF receptor mediates IGF-1-stimulated shc phosphorylation and ERK1/2 activation in COS-7 cells. J Biol Chem 2000;275:22583–9.
33. Lu Y, Zi X, Zhao Y, Mascarenhas D, Pollak M. Insulin-like growth factor-I receptor signaling and resistance to trastuzumab (Herceptin). J Natl Cancer Inst 2001;93:1852–7.
34. Lu Y, Zi X, Pollak M. Molecular mechanisms underlying IGF-I-induced attenuation of the growth-inhibitory activity of trastuzumab (Herceptin) on SKBR3 breast cancer cells. Int J Cancer 2004;108:334–41.
35. Jones HE, Goddard L, Gee JM, et al. Insulin-like growth factor-I receptor signalling and acquired resistance to gefitinib (ZD1839; Iressa) in human breast and prostate cancer cells. Endocr Relat Cancer 2004;11:793–814.
36. Chakravarti A, Loeffler JS, Dyson NJ. Insulin-like growth factor receptor I mediates resistance to anti-epidermal growth factor receptor therapy in primary human glioblastoma cells through continued activation of phosphoinositide 3-kinase signaling. Cancer Res 2002;62:200–7.
37. Steinbach JP, Eisenmann C, Klumpp A, Weller M. Co-inhibition of epidermal growth factor receptor and type 1 insulin-like growth factor receptor synergistically sensitizes human malignant glioma cells to CD95L-induced apoptosis. Biochem Biophys Res Commun 2004;321:524–30.
38. Mendelsohn J. The epidermal growth factor receptor as a target for cancer therapy. Endocr Relat Cancer 2001;8:3–9.
39. Sandler A. Clinical experience with the HER1/EGFR tyrosine kinase inhibitor erlotinib. Oncology (Williston Park) 2003;17:17–22.
40. Ready N. Inhibition of the epidermal growth factor receptor in combined modality treatment for locally advanced non-small cell lung cancer. Semin Oncol 2005;32:S35–41.
41. Hidalgo M. Erlotinib: preclinical investigations. Oncology (Williston Park) 2003;17:11–6.
42. Mitsiades CS, Mitsiades NS, McMullan CJ, et al. Inhibition of the insulin-like growth factor receptor-1 tyrosine kinase activity as a therapeutic strategy for multiple myeloma, other hematologic malignancies, and solid tumors. Cancer Cell 2004;5:221–30.
43. Warshamana-Greene GS, Litz J, Buchdunger E, Garcia-Echeverria C, Hofmann F, Krystal GW. The insulin-like growth factor-I receptor kinase inhibitor, NVP-ADW742, sensitizes small cell lung cancer cell lines to the effects of chemotherapy. Clin Cancer Res 2005;11:1563–71.
44. Hu YP, Dominguez I, Hauser J, et al. Characterization of *in vitro* and *in vivo* antitumor activity for novel IGF1R kinase inhibitors in colon cancer cells. Mol Cancer Ther 2007;6:3506–7s.
45. Black JD, Brattain MG, Krishnamurthi SA, Dawson DM, Willson JK. ErbB family targeting. Curr Opin Investig Drugs 2003;4:1451–4.
46. Adams TE, McKern NM, Ward CW. Signalling by the type 1 insulin-like growth factor receptor: interplay with the epidermal growth factor receptor. Growth Factors 2004;22:89–95.
47. Morgillo F, Woo JK, Kim ES, Hong WK, Lee HY. Heterodimerization of insulin-like growth factor receptor/epidermal growth factor receptor and induction of survivin expression counteract the antitumor action of erlotinib. Cancer Res 2006;66:10100–11.
48. Hu YP, Ji Q, Kan J, et al. The combination treatment with inhibitors targeting the type I insulin-like growth factor receptor and the epidermal growth factor receptor in human colon cancer [abstract 5073]. Annual Meeting of the American Association for Cancer Research, Washington, District of Columbia, 2006.
49. Barnes CJ, Ohshiro K, Rayala SK, El-Naggar AK, Kumar R. Insulin-like growth factor receptor as a therapeutic target in head and neck cancer. Clin Cancer Res 2007;13:4291–9.

Heterogeneity of Receptor Function in Colon Carcinoma Cells Determined by Cross-talk between Type I Insulin-like Growth Factor Receptor and Epidermal Growth Factor Receptor

Yi Peter Hu, Sandip B. Patil, Michelle Panasiewicz, et al.

Cancer Res 2008;68:8004-8013.